



Cite this: *Phys. Chem. Chem. Phys.*,  
2024, 26, 8651

# Quantifying hydroxyl radicals generated by a low-temperature plasma using coumarin: methodology and precautions†

Florent Ducrozet,<sup>a</sup> Amal Sebastian,<sup>ab</sup> Cecilia Julieta Garcia Villavicencio,<sup>ab</sup>  
Sylwia Ptasińska<sup>ab</sup> and Cécile Sicard-Roselli<sup>id</sup>\*<sup>c</sup>

The detection and quantification of hydroxyl radicals (HO•) generated by low-temperature plasmas (LTPs) are crucial for understanding their role in diverse applications of plasma radiation. In this study, the formation of HO• in the irradiated aqueous phase is investigated at various plasma parameters, by probing them indirectly using the coumarin molecule. We propose a quantification methodology for these radicals, combining spectrophotometry to study the coumarin reaction with hydroxyl radicals and fluorimetry to evaluate the formation yield of the hydroxylated product, 7-hydroxycoumarin. Additionally, we thoroughly examine and discuss the impact of pH on this quantification process. This approach enhances our comprehension of HO• formation during LTP irradiation, adding valuable insights to plasma's biological applications.

Received 4th January 2024,  
Accepted 24th February 2024

DOI: 10.1039/d4cp00040d

rsc.li/pccp

## 1. Introduction

Low-temperature plasmas (LTPs), often referred to as “cold plasmas”, are inquired in a field at the intersection of physics and chemistry and have emerged as a revolutionary tool with profound implications in areas of research such as material science, biomedicine, environmental remediation, and industrial processes. In strong contrast to the extreme temperatures typically associated with traditional plasmas, low-temperature plasmas operate at temperatures relevant to physiological processes, making them a gentle yet potent source of reactive species. As a result, the significance of LTPs in the field of biomedicine keeps increasing<sup>1–4</sup> as they offer non-invasive, precise, and versatile means to manipulate biological materials at the molecular level. From sterilization<sup>5</sup> and wound healing<sup>1</sup> to cancer treatment,<sup>2</sup> diverse and continually expanding applications of this remarkable technology are mainly based on radical production. Several studies reported that within LTPs, reactive nitrogen and oxygen species (RNOS) are generated.<sup>6,7</sup> Among them, hydroxyl radicals (HO•) stand out as one of the most oxidizing species known in aqueous media, with a redox

potential of 2.18 V *versus* normal hydrogen electrode.<sup>8</sup> These radicals are well-known to have a strong impact on biological media.<sup>9,10</sup> Their relevance in medicine and biology arises from their dual nature as a destructive agent contributing to cellular component damages such as DNA strand breaks and oxidative stress, and as a vital component in immune responses and therapeutic strategies. Understanding the role and regulation of HO• in biological systems is crucial for advancing our knowledge of disease processes, developing new treatments, and designing innovative interventions. Consequently, it is of primary importance to properly assess the impact of LTPs on irradiated biological targets and their medium, and therefore robust methods for quantifying these radicals are mandatory. As HO• possess a very short lifetime, close to 10<sup>−7</sup> s,<sup>11</sup> and a very low absorption capacity,<sup>12</sup> their direct detection in an aqueous medium is challenging for standard photo-absorption techniques. Hence, several strategies to indirectly detect these radicals were developed and include the use of molecular probes for electron paramagnetic resonance,<sup>13,14</sup> UV-Vis spectroscopy,<sup>15–17</sup> or fluorimetry.<sup>18,19</sup> Fluorescence detection presents the main advantage of being very sensitive. Hydroxyl radical fluorometric probes are usually aromatic compounds.<sup>13</sup> Among them, coumarin is a well-known sensitive and selective probe for HO• as it was already reported decades ago under ionizing radiation.<sup>20,21</sup> Hydroxyl radicals can react with several available sites of coumarin on both the benzenic and lactone rings (Scheme 1). This leads to the formation of several oxidized products and mainly hydroxycoumarins which are the most favorable to be formed, from 3- to 8-hydroxycoumarin. Among them, only 7-hydroxycoumarin (7-OHCou) possesses a high

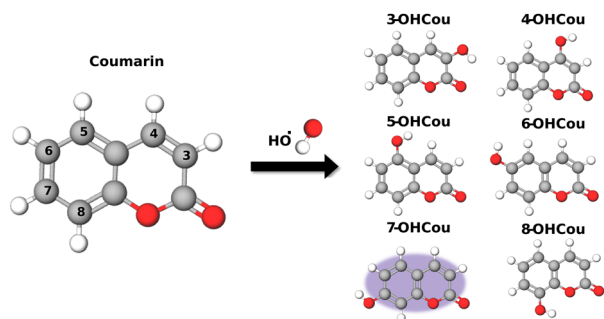
<sup>a</sup> Radiation Laboratory, University of Notre Dame, Notre Dame, IN 46556, USA.  
E-mail: florent.ducrozet@sorbonne-universite.fr, asebast1@nd.edu,  
cgarcavi@nd.edu, sylwia.ptasinska.1@nd.edu

<sup>b</sup> Department of Physics and Astronomy, University of Notre Dame, Notre Dame,  
IN 46556, USA

<sup>c</sup> Institut de Chimie Physique, UMR 8000, CNRS, Université Paris-Saclay,  
91405 Orsay, France. E-mail: cecile.sicard@universite-paris-saclay.fr

† Electronic supplementary information (ESI) available: Additional HPLC analysis of irradiated coumarin. See DOI: <https://doi.org/10.1039/d4cp00040d>





Scheme 1 Schematic representation of coumarin and its hydroxylated products.

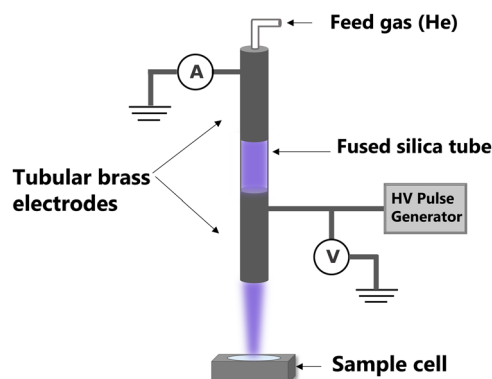
fluorescence yield,<sup>22</sup> allowing an indirect but sensitive detection of  $\text{HO}^\bullet$  by a simple fluorescence assay. Considering the numerous advantages of coumarin as a probe of  $\text{HO}^\bullet$ , it was applied for a large variety of systems such as exposition to ionizing radiation,<sup>20,23</sup> UV photolysis,<sup>24,25</sup> plasma irradiation,<sup>7,26</sup> sonication,<sup>27</sup> Fenton reaction<sup>28</sup> and also to biological hydroxylating systems.<sup>29</sup>

In the case of LTP irradiation, coumarin was already used as a  $\text{HO}^\bullet$  probe in only a few studies. Audemar *et al.* investigated plasma enrichment with  $\text{HO}^\bullet$  and tracked their production kinetics through 7-OH-Cou titration.<sup>7</sup> Additionally, Blatz *et al.* investigated the link between plasma parameters, such as voltage and frequency, and  $\text{HO}^\bullet$  formation dependence by measuring 7-OH-Cou fluorescence under several conditions.<sup>26</sup> Though both works reported 7-OH-Cou fluorescence intensities or concentration values, none of them converted both parameters into hydroxyl radical concentrations. Indeed, translating fluorescence intensities into accurate radical concentrations isn't straightforward because the formation yield of 7-OH-Cou among all coumarin oxidation products varies with irradiation systems and experimental conditions, as previously pointed out for coumarin<sup>22</sup> and coumarin-3-carboxylic acid.<sup>30</sup> Therefore, our goal here is to determine this yield and to determine  $\text{HO}^\bullet$  concentrations as the function of the plasma parameters. We will present a methodology to obtain an accurate quantification of hydroxyl radicals obtained upon LTP irradiation. Then, we will highlight the importance of controlling the pH value during the assay to ensure an accurate titration of 7-hydroxycoumarin.

## 2. Results and discussion

### Detection and quantification of hydroxyl radicals

The apparatus used for that study is a helium-fed atmospheric pressure LTP source, in which plasma is ignited based on a dielectric barrier discharge (Scheme 2). As already described,<sup>26</sup> many parameters impact the radicals' production by plasma, such as feed gas composition, flow rate, plasma voltage and frequency. In this study, helium was chosen as feed gas and the flow rate was fixed at 2 standard liters per minute (slm). Two irradiation conditions were tested which represent two extreme conditions of this particular plasma source, with different voltage/frequency combinations: 8 kV/1 kHz and 10 kV/4 kHz.



Scheme 2 Scheme of a LTP's set-up.

A sample cell containing an aqueous solution of 1.5 mM coumarin with 10 mM phosphate buffer with pH of 7 was irradiated at the two plasma conditions up to 90 s. Given the rate constant of coumarin with hydroxyl radicals ( $1.05 \times 10^{10} \text{ L mol}^{-1} \text{ s}^{-1}$ ),<sup>22</sup> these species react in *ca.* 65 ns. After irradiation, samples were analyzed using fluorescence spectroscopy with a 326 nm excitation light beam and 7-OH-Cou fluorescence emission was detected from 380 to 600 nm (Fig. 1). As expected, the fluorescence intensity increases proportionally with irradiation time with a maximum intensity at *ca.* 453 nm. To ensure that this fluorescence arises from the reaction between coumarin and  $\text{HO}^\bullet$ , another series of irradiations were performed in the presence of a high concentration of dimethylsulfoxide (DMSO), an efficient  $\text{HO}^\bullet$  scavenger (rate constant of  $6.6 \times 10^9 \text{ L mol}^{-1} \text{ s}^{-1}$ ).<sup>31</sup> In this case, no fluorescence signal attributed to 7-OH-Cou formation is detected (Fig. 1a), hence  $\text{HO}^\bullet$  reacting with DMSO.

The fluorescence intensity conversion into 7-OH-Cou concentration was performed using 7-OH-Cou standard solutions as a calibration. From Fig. 1b, the 7-OH-Cou formation yields are  $4.51 \pm 0.13$  and  $20.16 \pm 0.85 \text{ nM s}^{-1}$  for 8 kV/1 kHz and 10 kV/4 kHz conditions, respectively. Comparing both plasma conditions, higher voltage and frequency induce an increase by a factor 4.5 of the 7-OH-Cou formation yield. These results corroborate those of Blatz *et al.* who also reported an increase in  $\text{HO}^\bullet$  radicals formation using a dielectric barrier discharge-based LTP when increasing voltage and frequency.<sup>26</sup> In our previous work, we followed the formation of several reactive oxygen species (including  $\text{HO}^\bullet$  radicals) using a Fricke dosimeter<sup>32</sup> for irradiations at 8 kV/1 kHz and 10 kV/4 kHz. These results also presented an increased yield by a factor 3 between the two irradiation conditions, which is in relatively good agreement with the ratio of 7-OH-Cou formation yields for both conditions measured here.

As already mentioned, previous works revealed different ratios of 7-OH-Cou among the different hydroxycoumarin isomers, depending on the irradiation modalities or dose rates.<sup>22,29,33</sup> This detection of different isomers as products of irradiation is also reported in the present study in Fig. 2. This figure shows a comparison of chromatographic profiles of irradiated coumarin with LTP and gamma-rays. It can be



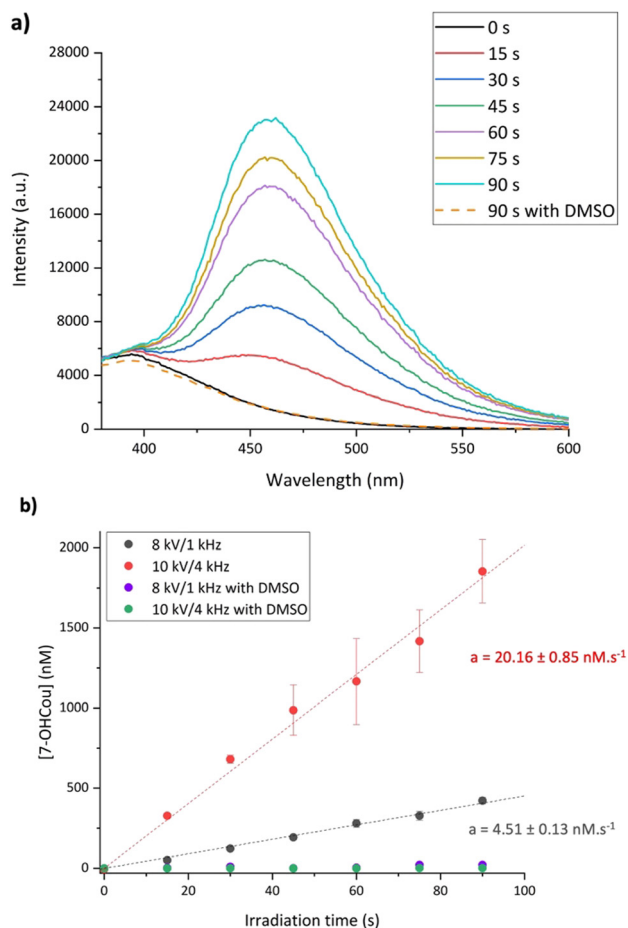


**Fig. 1** (a) 7-OH-Cou fluorescence spectra for several irradiation times up to 90 s at 10 kV/4 kHz, (b) evolution of the 7-OH-Cou concentration with the irradiation time at 8 kV/1 kHz and 10 kV/4 kHz in the presence or absence of DMSO. All samples are buffered at pH 7. In the absence of DMSO, the data represent the average of three independent experiments.

noticed that, for both types of radiation, 5-, 6-, 7- and 8-hydroxycoumarin are formed with respective retention time of 19.4, 21.3, 21.6 and 22.9 min, which is in agreement with standard molecule injections and previous chromatographic experiments.<sup>22,34,35</sup> 3- and 4-hydroxycoumarin, if formed, are below the detection limit, which was also reported for photolysis and radiolysis of coumarin aqueous solutions, probably due to unfavorable electronic configuration on the lactone ring.<sup>22,24,33</sup> Based on the results in Fig. 2, it can be concluded that the same hydroxycoumarin isomers are formed and their quantity increases with the irradiation time, attesting for a growing production of HO• with irradiation time and/or dose. However, the ratio between these different hydroxylation products is distinct for LTP and gamma-ray irradiation. As already reported, regioselectivity for coumarin hydroxylation depends on the type of radiation.<sup>34–36</sup> Indeed, it can be observed that for LTP irradiation, 6-OH-Cou presents the highest signal whereas for gamma-ray irradiation the highest contribution corresponds to 5-OH-Cou. Furthermore, the same hydroxycoumarins ratios is observed for 8 kV/1 kHz and 10 kV/4 kHz irradiations (Fig. S1, ESI†).

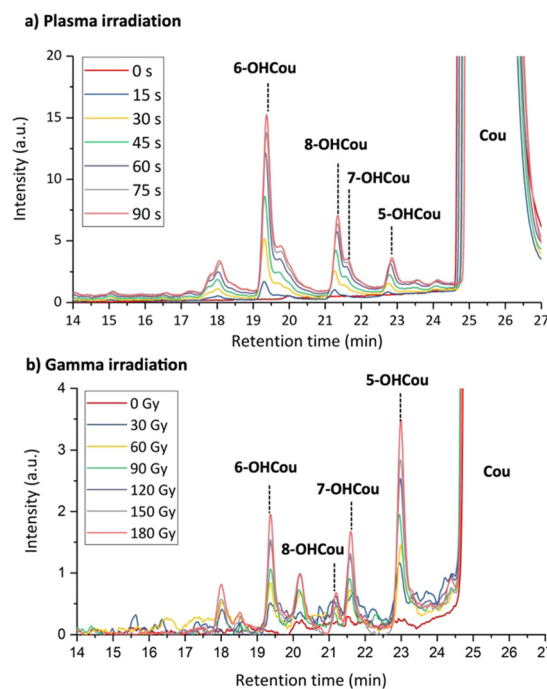


**Fig. 2** HPLC profiles of buffered coumarin solutions irradiated by: (a) plasma at 10 kV/4 kHz; and (b) gamma-rays. Detection was performed by absorption at 280 nm.

The different product ratios indicate that the conversion of 7-OH-Cou concentration into HO• concentration cannot be realized by a simple analogy with ionizing radiation or another hydroxylating process. To overcome that issue, we choose to compare the reaction yield of coumarin and the formation yield of 7-OH-Cou as a function of the irradiation time. Indeed, spectrophotometry allows us to determine this coumarin reaction yield by measuring its absorption decrease.

To validate this strategy, we first applied it to samples irradiated by gamma radiation for which hydroxyl radical formation yield is well-known.<sup>37</sup> Fig. 3a represents the coumarin concentration as a function of the dose, calculated by Beer-Lambert's law from absorption measurements. As expected, the coumarin concentration decreases with the irradiation dose, due to its reaction with HO•. The obtained reaction yield is  $ca. -250 \pm 40 \text{ nmol J}^{-1}$  which is in very good agreement with the tabulated HO• formation value of  $280 \text{ nmol J}^{-1}$  (equivalent to  $\text{nM Gy}^{-1}$ ). This result indicates that for a gamma-ray irradiation of 1.5 mM coumarin solution,  $ca. 90\%$  of the hydroxyl radicals formed react with coumarin. Here, absorption spectroscopy appears as a suitable technique to monitor HO• production through coumarin reaction, despite of being less sensitive than fluorescence. However, the latter allows us to extract the corresponding formation yield of 7-OH-Cou (Fig. 3b) which is  $ca. 9.14 \pm 0.20 \text{ nmol J}^{-1}$ . This value is in the same order of magnitude as the one obtained elsewhere by gamma-ray irradiation ( $^{137}\text{Cs}$  source).<sup>22</sup> Calculating the ratio between the coumarin decrease and 7OH-Cou increase, we obtain a value of  $ca. 3.7\%$  which means that one 7-OH-Cou molecule will be formed for  $ca. 27$  reactions between coumarin



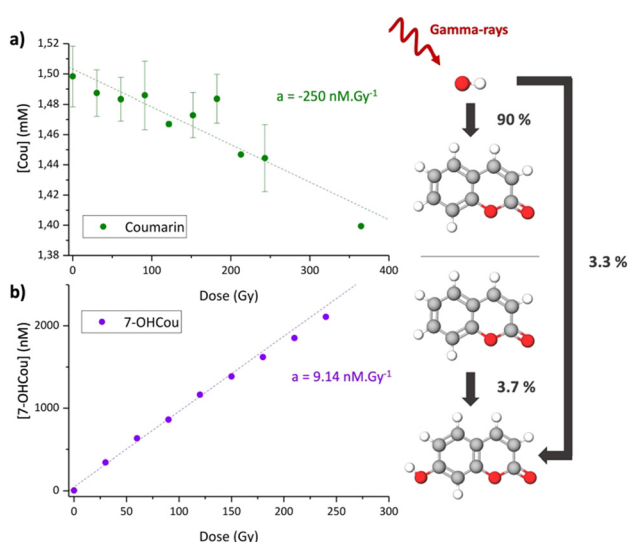


Fig. 3 (a) Coumarin concentration probed by absorption spectroscopy and (b) 7-OH-Cou concentration probed by fluorescence, both as a function of the gamma irradiation dose. For absorption, the data points represent the average of two independent experiments.

and hydroxyl radicals generated in the aqueous phase. Knowing the formation yield of  $\text{HO}^\bullet$  under gamma-rays, this result can be also interpreted as 3.3% of generated  $\text{HO}^\bullet$  are forming the fluorescent 7-OH-Cou. This percentage is very close to the one estimated for X-ray irradiation with a similar initial concentration of coumarin.<sup>23</sup>

Taking that into consideration, identical absorption measurements were performed on coumarin samples irradiated by LTP (Fig. 4). First, no significant decrease in the coumarin signal during irradiation in the presence of DMSO confirms that coumarin is only reacting with hydroxyl radicals and not with other RNOS emitted or produced by the LTP source.

For the 10 kV/4 kHz condition, the obtained value for coumarin reaction is  $-1.8 \pm 0.2 \mu\text{M s}^{-1}$ . Considering that 90% of hydroxyl radicals react with coumarin, we can conclude that this plasma irradiation condition leads to the formation of *ca.*  $2.02 \pm 0.09 \mu\text{M}$  of  $\text{HO}^\bullet$  within one second. From Fig. 1 and the yield of formation of 7-OH-Cou of  $20.14 \text{ nM s}^{-1}$  for the same plasma conditions, we can calculate that the 7-OH-Cou represents only 1% of the  $\text{HO}^\bullet$  radicals brought by the LTP in the aqueous phase. This value corroborates the HPLC profile (Fig. 2) where 7-OH-Cou signal contribution is much lower for plasma compared to gamma irradiation. Considering this percentage, we can extract from Fig. 1b the formation yield of hydroxyl radicals for 8 kV/1 kHz to be  $0.45 \pm 0.01 \mu\text{M s}^{-1}$ .

The obtained yields of hydroxyl radicals at different plasma conditions confirm our previous postulations of increase in reactive species formation with higher voltage and frequency as we deduced based on the experiments on DNA damage induced by LTP, for which direct measurement of  $\text{HO}^\bullet$  was not possible.<sup>38,39</sup>

### Influence of pH

The quantification of hydroxyl radicals as described above was conducted in the presence of 10 mM phosphate buffer at pH 7.

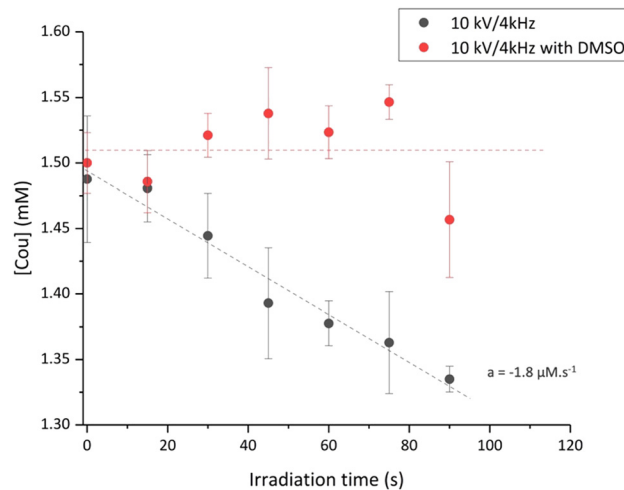


Fig. 4 Coumarin concentration probed by absorption spectroscopy for plasma irradiation at 10 kV/4 kHz with and without DMSO. The data points represent the average of two independent experiments.

One can wonder about the possibility of performing the same quantification in a simple unbuffered aqueous sample. To test such a condition, an aqueous solution of coumarin was irradiated with the same plasma parameters in the absence of buffer. Fig. 5a shows the increase in fluorescence intensities for several plasma irradiation times in unbuffered coumarin solutions. Interestingly, the expected signal from 7-OH-Cou has its maximum red-shifted to 470 nm. To ensure that this different maximum wavelength does not arise from a different oxidation product of coumarin, we performed an HPLC analysis of the corresponding samples (Fig. 5b). The chromatographic pattern, similar to the one of the irradiated buffered samples, confirms that the increasing fluorescence signal detected at 470 nm corresponds to 7-OH-Cou.

Several parameters can induce a fluorescence shift, such as solvent composition, temperature, or pH. As already described in the literature, a fluorescence shift of 7-OH-Cou to higher wavelengths can result from a decrease in the solution's pH as the fluorescence of protonated and deprotonated forms of 7-OH-Cou differs.<sup>27,40</sup> Also, several studies have demonstrated that the pH of water irradiated by LTPs is lowered due to the introduction of protons, most apparently by the formation of nitric and peroxynitrous acids by the radical species emitted by the plasma itself.<sup>6,41</sup> Additionally, it was reported that the pH drop is dependent on the plasma conditions.<sup>42,43</sup> Therefore, we also measured the variation of pH after irradiation under both LTP conditions (Fig. 6a). The initial pH value is *ca.* 6.1, which is the common pH of unbuffered ultrapure water. With increasing irradiation time, a decrease in pH is observed. As expected, this pH modification is higher for irradiation at 10 kV/4 kHz than at 8 kV/1 kHz. Converting pH to  $\text{H}^+$  concentration, the introduction of protons appears proportional to the irradiation time (Fig. 6b). The linear trend until 120 s for both plasma conditions allows us to extract  $\text{H}^+$  formation yields of  $0.18 \pm 0.01 \mu\text{M s}^{-1}$  and  $1.35 \pm 0.04 \mu\text{M s}^{-1}$  at 8 kV/1 kHz and 10 kV/4 kHz, respectively.





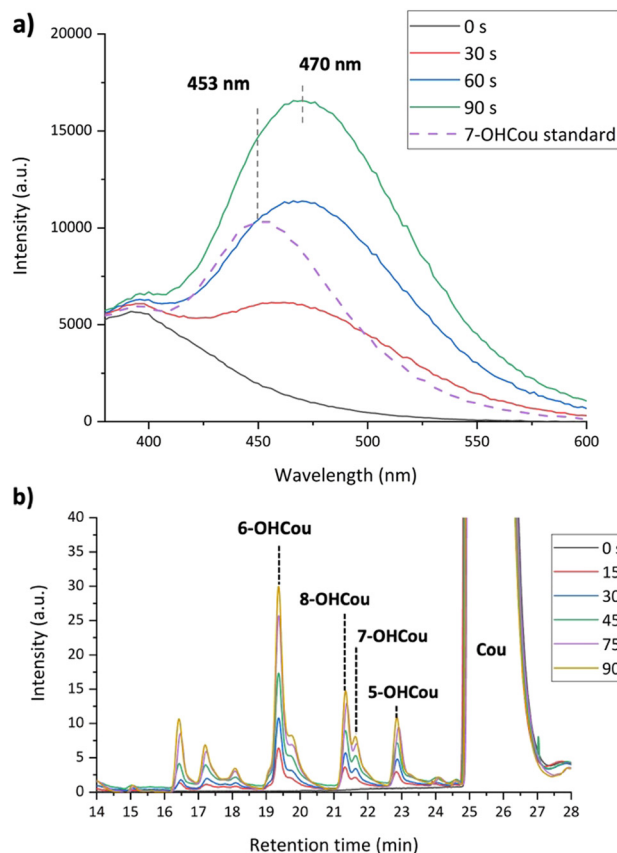


Fig. 5 (a) 7-OHCOu fluorescence spectra of irradiated coumarin samples up to 90 s at 8 kV/1 kHz (unbuffered) and 7-OHCOu standard in ultrapure water; (b) HPLC profile of unbuffered solutions irradiated by plasma at 10 kV/4 kHz. Detection by absorption at 280 nm.

This pH changes with irradiation time may lead to an inaccurate quantification of 7-OHCOu. Indeed, these observations highlighted the fact that the calibration curve of a 7-OHCOu standard solution must be recorded at the same pH as the sample since the pH varies for each unbuffered sample causing the prevention of an accurate calibration of 7-OHCOu concentration.

In addition,  $pK_a$  values of hydroxycoumarins were already the focus of different studies<sup>40,44,45</sup> where it was demonstrated that the negative charge of the different phenolate anions varies strongly with the position of the hydroxyl group on the coumarin ring. A  $pK_a$  of 7.6 was determined for the 7-OHCOu molecule which implies that both protonated and deprotonated forms of 7-OHCOu are present in buffered solution at neutral pH. This is illustrated in Fig. 7 which shows the excitation spectrum of plasma irradiated coumarin in the presence or absence of buffer.

For the unbuffered sample after 90 s of plasma treatment, the pH is downshifted to 3.9 (Fig. 6a). This pH value ensures the presence of only the protonated 7-OHCOu form that appears to possess a maximum intensity for excitation at ca. 340 nm (Fig. 7). For the buffered sample, two contributions are observed at 340 and 370 nm illustrating an acido-basic equilibrium between protonated and deprotonated form, in agreement with previous

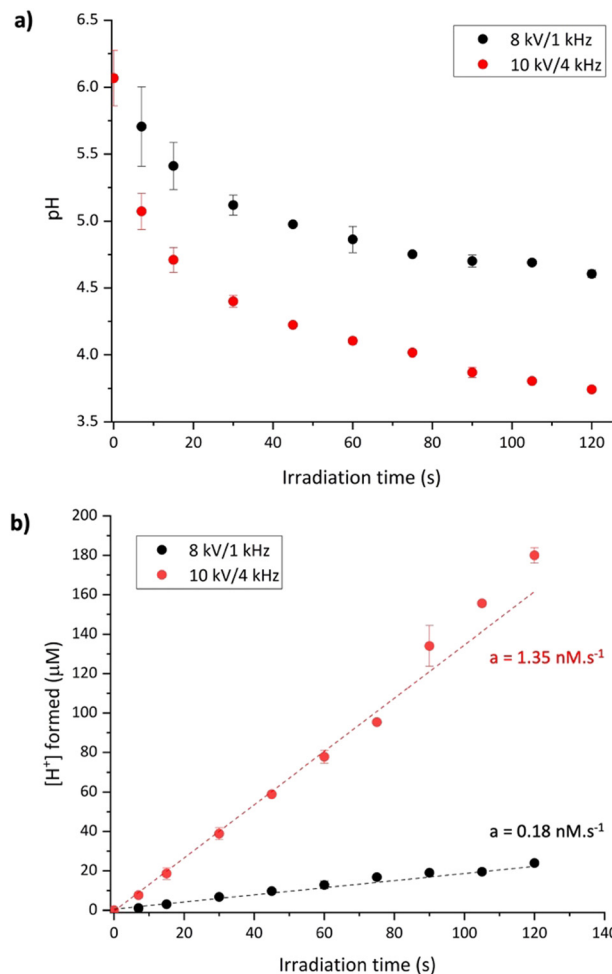


Fig. 6 (a) pH evolution of water as a function of irradiation time for the 8 kV/1 kHz and 10 kV/4 kHz conditions. 2 trials for each irradiation were realized; (b) evolution of the concentration of protons formed as a function of irradiation time. All data points represent the average of two independent experiments.

works.<sup>40</sup> Coexistence of these two 7-OHCOu protonation states corroborates Fig. 5. Indeed, fluorescence maximum is upshifted with decreasing pH, with a maximal fluorescence at 470 nm for the protonated form. Thus, we can conclude that any hydroxyl radical quantification with coumarin requires a calibration with standard 7-OHCOu recorded at a fixed pH, which implies the mandatory use of buffers for LTP irradiation.

### 3. Experimental

#### 3.1. Materials.

Coumarin (purity >99%) was purchased from Sigma-Aldrich. 7-Hydroxycoumarin (7-OHCOu, purity 98%) was purchased from Thermoscientific. Dimethyl sulfoxide (DMSO, purity >99.7%), sodium phosphate dibasic, and sodium phosphate monobasic were purchased from Fisher Scientific. Phosphate buffer was prepared at pH 7 using  $\text{Na}_2\text{HPO}_4$  and  $\text{NaH}_2\text{PO}_4$  solutions.



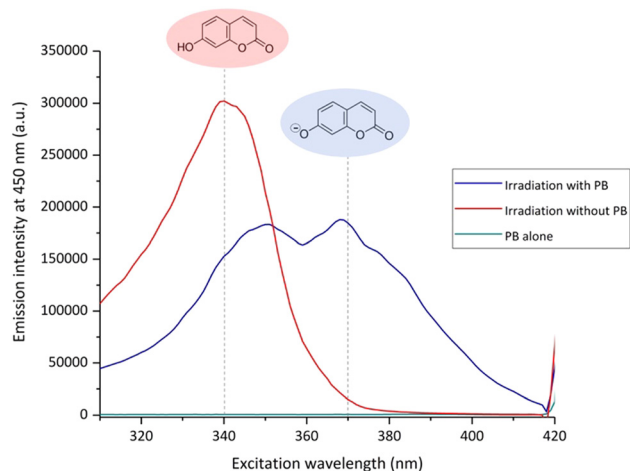


Fig. 7 Excitation spectra of coumarin samples irradiated for 90 s at 10 kV/4 kHz in the presence or absence of buffer and the buffer alone. Spectra for emission at 450 nm.

For irradiation experiments, a 1.5 mM coumarin aqueous solution in 10 mM buffer was prepared. For some experiments, 1 M of DMSO was added to the solutions. All aqueous solutions and dilutions were made using ultrapure water (18.2 MΩ cm resistivity) and kept refrigerated between experiments.

### 3.2. Low-temperature plasma irradiation

The plasma irradiation, ignited based on dielectric-barrier discharge, was performed using a helium-fed (purity of 99.999%) atmospheric pressure LTP source. The plasma source consisted of a fused silica capillary inserted into two tubular brass electrodes with a length of 50 mm. The bottom electrode was powered by high voltage squared pulses generated by a DC power supply, while the top electrode was grounded. The helium flow was adjusted to 2 slm using a flow controller (Bronkhorst High-tech) and plasma was ignited inside the tube between both electrodes. A complete description of LTP set-up and systematic characterization of plasma were previously reported.<sup>46,47</sup>

Irradiation was performed under two conditions of voltage and frequency combinations, that is 8 kV at 1 kHz and 10 kV at 4 kHz. The maximum discharge current recorded at the rising edge of the voltage pulse was 40 mA for 8kV/1kHz and 125 mA for 10 kV/4 kHz. At each condition, samples prepared in the same way were irradiated at least three times. After irradiation samples were taken for further analysis.

### 3.3. Gamma-rays irradiation

Gamma irradiation experiments were performed using a panoramic <sup>60</sup>Co source (IL60PL Cis-Bio International, photons of 1.17 and 1.33 MeV) with dose rates of *ca* 5 Gy min<sup>-1</sup> depending on the chosen distance from the gamma source. Dosimetry was determined using a Fricke dosimeter.<sup>48</sup>

### 3.4. Fluorescence measurements

Formation of 7-OHCOu was quantified post-irradiation by fluorescence with excitation at 326 nm and the maximum of

emission detected at 453 nm. Calibration was realized using the same protocol with 7-OHCOu standard solutions. Fluorescence measurements were recorded with an Infinite 200 Pro microplate reader (Tecan Group Ltd, Switzerland).

### 3.5. Chromatography analysis

Coumarin and hydroxycoumarins were analyzed by HPLC (HP 1100 Series, Agilent), and hydrophobic separation was performed on a C18 column (250 × 4.6 mm, and 5 μm particle diameter). 100 μL were injected. Mobile phases are A: (89% water, 10% methanol, and 2.5% acetic acid) and B: (89% methanol, 10% water and 2.5% acetic acid). Gradient elution is 0% B over 5 min, 0–30% B in 5 min, 30–50% B in 20 min, and 50–100% B in 5 min, with a flow rate of 0.8 mL min<sup>-1</sup>. Absorbance detection was realized at 280 nm. Peaks were attributed as labeled by comparison to standard hydroxycoumarins injected under the same chromatographic conditions. Chromatograms were realigned to the 6-hydroxycoumarin peak and baseline corrections were applied when necessary.

## Conclusions

In conclusion, this study has intricately explored the detection and quantification of hydroxyl radicals generated by low-temperature plasmas, employing a comprehensive approach combining fluorescence, spectrophotometry, and HPLC techniques. The results highlight the exceptional efficiency of the employed plasma conditions in producing a significant quantity of HO•. A quantification methodology of these radicals was presented along with the importance of pH control during that process. Indeed, this study warned about the necessity for cautious interpretation when quantifying HO• using coumarin fluorescence, given the susceptibility of the 7-OHCOu formation yield to various irradiation parameters, as exemplified by the pH of the sample solution. The establishment of a reliable strategy for quantifying LTP-originating hydroxyl radicals is imperative for gaining comprehensive insights into plasma-induced biochemical interactions, addressing a notable gap in understanding apparent in previous studies. This research contributes significantly to the refinement of methodologies, thereby advancing our understanding of the complex dynamics involved in plasma-induced biochemical processes.

## Author contributions

All authors participated in the investigation, analysis, and writing of the draft.

## Conflicts of interest

The authors declare no conflict of interest.



## Acknowledgements

The authors would like to thank James Beauvil (Institut de Chimie Physique, CNRS UMR 8000, Université Paris-Saclay, Orsay, F-91405, France) for technical assistance during gamma irradiation and acknowledge the U.S. Department of Energy Office of Science, Office of Basic Energy Sciences under Award Number DE-FC02-04ER15533 (NDRL no: 5419).

## Notes and references

- 1 D. B. Graves, *Phys. Plasmas*, 2014, **21**, 080901.
- 2 K. Arjunan, V. Sharma and S. Ptasińska, *IJMS*, 2015, **16**, 2971–3016.
- 3 M. Schuster, C. Seebauer, R. Rutkowski, A. Hauschild, F. Podmelle, C. Metelmann, B. Metelmann, T. Von Woedtke, S. Hasse, K.-D. Weltmann and H.-R. Metelmann, *J. Cranio-Maxillofac. Surg.*, 2016, **44**, 1445–1452.
- 4 E. Alizadeh and S. Ptasińska, *Biophysica*, 2021, **1**, 48–72.
- 5 S. Gershman, M. B. Harreguy, S. Yatom, Y. Raitses, P. Efthimion and G. Haspel, *Sci. Rep.*, 2021, **11**, 4626.
- 6 R. Thirumdas, A. Kothakota, U. Annapure, K. Siliveru, R. Blundell, R. Gatt and V. P. Valdramidis, *Trends Food Sci. Technol.*, 2018, **77**, 21–31.
- 7 M. Audemar, O. Vallcorba, I. Peral, J.-S. Thomann, A. Przekora, J. Pawlat, C. Canal, G. Ginalska, M. Kwiatkowski, D. Duday and S. Hermans, *Catal. Sci. Technol.*, 2021, **11**, 1430–1442.
- 8 W. H. Koppenol and J. Butler, *Adv. Free Radical Biol. Med.*, 1985, **1**, 91–131.
- 9 M. J. Davies and R. T. Dean, *Radical-Mediated Protein Oxidation: From Chemistry to Medicine*, 1997, vol. 74.
- 10 C. Von Sonntag, *Free-Radical-Induced DNA Damage and Its Repair: A Chemical Perspective*, 1989, vol. 40.
- 11 M. P. Lesser, *Annu. Rev. Physiol.*, 2006, **68**, 253–278.
- 12 H. Herrmann, *Chem. Rev.*, 2003, **103**, 4691–4716.
- 13 I. Rosenthal, C. M. Krishna, G. C. Yang, T. Kondo and P. Riesz, *FEBS Lett.*, 1987, **222**, 75–78.
- 14 R. P. Mason and K. T. Knecht, *Methods Enzymol.*, 1994, **233**, 112–117.
- 15 S. Singh and R. C. Hider, *Anal. Biochem.*, 1988, **171**, 47–54.
- 16 O. I. Aruoma, *Methods in Enzymology*, Elsevier, 1994, **233**, pp. 57–66.
- 17 G. Albarran and R. H. Schuler, *Radiat. Phys. Chem.*, 2003, **67**, 279–285.
- 18 W. A. Armstrong and D. W. Grant, *Can. J. Chem.*, 1960, **38**, 845–850.
- 19 R. W. Matthews, *Radiat. Res.*, 1980, **83**, 27.
- 20 K. Gopakumar, U. R. Kini, S. C. Ashawa, N. S. Bhandari, G. U. Krishnan and D. Krishnan, *Radiat. Eff.*, 1977, **32**, 199–203.
- 21 P. J. Creaven, D. V. Parke and R. T. Williams, *Biochem. J.*, 1965, **96**, 390–398.
- 22 G. Louit, S. Foley, J. Cabillie, H. Coffigny, F. Taran, A. Valleix, J.-P. Renault and S. Pin, *Radiat. Phys. Chem.*, 2005, **72**, 119–124.
- 23 C. Sicard-Roselli, E. Brun, M. Gilles, G. Baldacchino, C. Kelsey, H. McQuaid, C. Polin, N. Wardlow and F. Currell, *Small*, 2014, **10**, 3338–3346.
- 24 W. J. McCormick, C. Rice, D. McCrudden, N. Skillen and P. K. J. Robertson, *J. Phys. Chem. A*, 2023, **127**, 5039–5047.
- 25 H. Czili and A. Horváth, *Appl. Catal., B*, 2008, **81**, 295–302.
- 26 J. M. Blatz, D. Benjamin, F. A. Choudhury, B. B. Minkoff, M. R. Sussman and J. L. Shohet, *J. Vac. Sci. Technol., A*, 2020, **38**, 043001.
- 27 K. Hirano and T. Kobayashi, *Ultrason. Sonochem.*, 2016, **30**, 18–27.
- 28 F. Jean-M, D. B. Xochitl and S. Mika, *RSC Adv.*, 2018, **8**, 5321–5330.
- 29 L. B. Von Weymarn and S. E. Murphy, *Chem. Res. Toxicol.*, 2001, **14**, 1386–1392.
- 30 T. Kusumoto, H. Kitamura, S. Hojo, T. Konishi and S. Kodaira, *RSC Adv.*, 2020, **10**, 38709–38714.
- 31 G. V. Buxton, C. L. Greenstock, W. P. Helman and A. B. Ross, *J. Phys. Chem. Ref. Data*, 1988, **17**, 513–886.
- 32 E. R. Adhikari, V. Samara and S. Ptasińska, *Biol. Chem.*, 2018, **400**, 93–100.
- 33 G. Žerjav, A. Albrecht, I. Vovk and A. Pintar, *Appl. Catal., A*, 2020, **598**, 117566.
- 34 M. Gilles, E. Brun and C. Sicard-Roselli, *J. Colloid Interface Sci.*, 2018, **525**, 31–38.
- 35 E. Brun, H. A. Girard, J.-C. Arnault, M. Mermoux and C. Sicard-Roselli, *Carbon*, 2020, **162**, 510–518.
- 36 F. Ducrozet, E. Brun, H. A. Girard, J.-C. Arnault and C. Sicard-Roselli, *J. Phys. Chem. C*, 2023, **127**(39), 19544–19553.
- 37 H. A. Schwarz, *J. Phys. Chem.*, 1992, **96**, 8937–8941.
- 38 A. Sebastian, D. Spulber, A. Lisouskaya and S. Ptasińska, *Sci. Rep.*, 2022, **12**, 18353.
- 39 A. Sebastian, D. Lipa and S. Ptasińska, *ACS Omega*, 2023, **8**, 1663–1670.
- 40 D. W. Fink and W. R. Koehler, *Anal. Chem.*, 1970, **42**, 990–993.
- 41 R. Ma, G. Wang, Y. Tian, K. Wang, J. Zhang and J. Fang, *J. Hazard. Mater.*, 2015, **300**, 643–651.
- 42 P. Bruggeman and C. Leys, *J. Phys. D: Appl. Phys.*, 2009, **42**, 053001.
- 43 Y. Tian, R. Ma, Q. Zhang, H. Feng, Y. Liang, J. Zhang and J. Fang, *Plasma Process. Polym.*, 2015, **12**, 439–449.
- 44 H. K. Arora, A. R. Aggarwal and R. P. Singh, *Ind. J. Chem.*, 1982, **21A**, 844.
- 45 P. M. Nowak, M. Woźniakiewicz, M. Piwowarska and P. Kościelniak, *J. Chromatogr. A*, 2016, **1446**, 149–157.
- 46 E. R. Adhikari, V. Samara and S. Ptasińska, *J. Phys. D: Appl. Phys.*, 2018, **51**, 185202.
- 47 V. Samara, Y. Sutton, N. Braithwaite and S. Ptasińska, *Eur. Phys. J. D*, 2020, **74**, 169.
- 48 H. Fricke and S. Morse, *London, Edinburgh Dublin Philos. Mag. J. Sci.*, 1929, **7**, 129–141.

